Microbial Biotechnology

WILEY

MICROBIAL BIOTECHNOLOGY Open Access

RESEARCH ARTICLE OPEN ACCESS

The Metabolic and Physiological Responses to Spaceflight of a Lipopeptide-Producing *Bacillus subtilis*

Wan-Qi Qin[1] | Yi-Fan Liu[1,2] | Jin-Feng Liu[3] | Lei Zhou[1] | Shi-Zhong Yang[1,2] | Ji-Dong Gu[4] | Bo-Zhong Mu[1,2]

[1]State Key Laboratory of Bioreactor Engineering and School of Chemistry and Molecular Engineering, East China University of Science and Technology, Shanghai, P. R. China | [2]Shanghai Collaborative Innovation Center for Biomanufacturing Technology, Shanghai, P. R. China | [3]Daqing Huali Biotechnology Co., Ltd, Daqing, Heilongjiang, P. R. China | [4]Environmental Science and Engineering Group, Guangdong Technion Israel Institute of Technology, Shantou, Guangdong, P. R. China

Correspondence: Bo-Zhong Mu (bzmu@ecust.edu.cn)

Received: 22 June 2024 | **Revised:** 8 January 2025 | **Accepted:** 3 February 2025

Funding: This work was supported by the Fundamental Research Funds for the Central Universities of China, the National Key Research and Development Program of China (No. 2022YFC2105200) and the Research Program of the State Key Laboratory of Bioreactor Engineering.

Keywords: *Bacillus subtilis* | lipopeptide | molecular regulation | secondary metabolism | spaceflight | transcriptomics

ABSTRACT

Outer space is an extreme environment and the survival of many microorganisms after spaceflight is well established. However, adaptations of *Bacillus subtilis* to space stress, particularly metabolism, are largely unknown. Here, we first performed a spaceflight mission of the *B. subtilis* TD7 strain and compared the spaceflight-exposed strain with the wild-type in terms of their phenotype, biofilm formation and secondary metabolism. The spaceflight-exposed strain exhibited slower growth, different morphology and decreased biofilm formation. Importantly, a decline in lipopeptide production was observed after spaceflight. Multi-omics approaches were used to uncover the molecular mechanisms underlying secondary metabolism and 997 differentially expressed genes (DEGs) were found, involving the TCA cycle, fatty acid degradation, amino acid biosynthesis and quorum sensing systems. Further analysis of 26 lipopeptide-related DEGs further elucidated the relationship between the space environment and secondary metabolism regulation. Our findings could contribute to a better understanding of the relationship between the space environment and microbial adaptation mechanisms.

1 | Introduction

Outer space is a harsh environment with extreme vacuum, microgravity, a weak magnetic field, cosmic radiation, temperature fluctuation and high ultraviolet radiation, which has received great attention in recent years (Cockell et al. 2011; Huang et al. 2018). To date, with the rapid advancement of aerospace technology, the International Space Station (ISS) and low Earth orbit missions provide a suitable opportunity for astrobiology research and make it possible to exploit these environmental factors that are not easily accessible on Earth (Bijlani et al. 2021; Ott et al. 2020). There is considerable evidence that microorganisms can adapt to the space environment by altering phenotypic and genotypic characteristics, such as cell growth (Coil et al. 2016), biofilm formation (Daniela et al. 2019), virulence (Lam et al. 1998), metabolism (Huang et al. 2015), oxidative stress (Abshire et al. 2016) and gene expression (Mora et al. 2019). Although it has been reported for more than 60 years how microorganisms modify their physiological properties in response to the space environment, our knowledge of the molecular mechanisms is still unclear. Thus, comprehensive phenotypic experiments and omics analysis will provide new insights to better understand the microbial responses and mechanisms after space exposure.

Wan-Qi Qin and Yi-Fan Liu contributed equally to this study.

Among microbial candidates for space experiments, *Bacillus* species possess numerous remarkable characteristics that allow them to survive in adverse environments, including endospore formation and excellent metabolic ability (Dergham et al. 2023; Juhas and Ajioka 2017; Krüger et al. 2022). *B. subtilis* is a metabolically active bacterium that is widely present in the environment. Among many secondary metabolites of *B. subtilis*, lipopeptide has been widely applied in oil recovery, cosmetics, food and pharmaceutical industries (Wu et al. 2019). As a well-known cyclic lipopeptide, surfactin, composed of a fatty acid chain and a circular heptapeptide, is one of the most powerful biosurfactants with a variety of surface-active and bioactive properties, such as surface tension reduction, antimicrobial, antiviral and anticancer (Sani et al. 2024). In addition, surfactin is biosynthesised by nonribosomal peptide synthetases (NRPSs), which is a complex multienzyme composed of an adenylation domain for amino recognition and activation, a thiolated domain for the transportation of amino acids and peptide chains and a condensation domain for the formation of peptide bonds (Yang et al. 2020). However, there are still many hurdles in the continued development of lipopeptide that need to be overcome, including low production, a complex metabolic network and precursor requirements (Lu et al. 2019; Oikawa et al. 2022). Thus, it seems to be essential to carry out more research on its complex metabolic network and strict synthetic pathway, as these biosynthesis metabolisms are behind the adaptation.

In the present study, a wild-type *Bacillus subtilis* strain was sent into space carried by a Chinese spacecraft named XZF-SC (Xinyidai Zairen Feichuan—Shiyan Chuan, 'New Generation Crewed Spaceship - Test Ship') to explore the potential impact of complex space environmental factors inside the spacecraft. Here, we investigated the phenotypic characteristics, growth and biofilm formation ability of both the wild-type and spaceflight-exposed strains. The metabolic comparison has focused on an important metabolite lipopeptide. Next, a comparative transcriptomic analysis was performed to provide molecular evidence for the multifaceted response to spaceflight, revealing the significantly differential expressed genes and metabolic pathways. For the first time, this work presents a global response of *B. subtilis* strain to the space environment, and identifies significantly regulated genes and pathways related to secondary metabolism, revealing the intrinsic mechanism of spaceflight effect in secondary metabolism. Hence, these results will lay a theoretical foundation for future astrobiology studies of the relationship between microbial metabolism and the space environment.

2 | Experimental Procedures

2.1 | Bacterial Strain and Culture Conditions

The wild-type *B. subtilis* TD7 strain was isolated from the formation water of Chinese oil fields, which was used for both spaceflight and ground experiments (Mu et al. 2021). Routine cultivation was carried out in a basal Lysogeny Broth (LB) medium. *B. subtilis* grown to optical density at 600 nm (OD_{600}) of 1.0 was used as the inoculum for all experiments unless otherwise mentioned.

2.2 | Spaceflight Mission

The wild-type strain was cultured to the logarithmic growth phase in the laboratory and stored in a cryotube containing 1.5 mL of glycerol-LB medium (1×10^7 CFU/mL). Then, all biological samples were sent to Beijing and uniformly stored in a specific fixed test device inside the return capsule, which was launched into outer space by the maiden Long March 5B (CZ-5B) rocket launching the XZF-SC (Xinyidai Zairen Feichuan—Shiyan Chuan, 'New Generation Crewed Spaceship - Test Ship'). The XZF-SC was launched at 6:00 pm (GMT + 8) on 5 May, 2020, at Wenchang Space Launch Center on the coast of south China's Hainan Province. After a flight of 488 s, the launch vehicle CZ-5B put the spacecraft into a low earth orbit, and then, it was raised to about 8000 km after seven autonomous orbit changes. On 8 May, 2020, 12:21 AM (GMT + 8), the re-entry module went into returned orbit and landed safely at the Dongfeng landing site at 1:49 pm (GMT + 8). On 29 May, the return capsule of the new manned spacecraft test ship was unpacked in Beijing. Our bacterial fluids were sent to the laboratory and frozen at −80°C.

2.3 | Morphological Analysis

The morphology of the wild-type (BSG) and spaceflight-exposed (BSS) strains was observed by scanning electron microscope (SEM). After incubating for 12 h at 37°C, bacterial cells were obtained by centrifuging at 5000 rpm for 10 min. This was followed by three washings in the PBS (0.1 M phosphate buffer solution) for 15 min to remove impurities, and the cells were fixed with 2.5% glutaraldehyde solution at 4°C overnight. The samples were dehydrated by a graded series of ethanol solutions (30%, 50%, 70%, 85%, 95% and 100%) for 15 min at each step. The samples were then critical point dried and coated with gold–palladium. In the end, the samples were sent to the East China University of Science and Technology for SEM analysis (Helios G4 UC SEM).

2.4 | Phenotypic and Biochemical Analysis

The strains were grown on LB-agar plates, colony characters were noted and morphology was detected by microscopic observation and Gram staining. Both strains were tested for salt, pH and temperature tolerance to determine growth. In addition, sugar fermentation tests were also performed, containing sucrose, maltose, glucose, methanol, mannitol, D-fructose, lactose, galactose, xylose and other common sugars. Other biochemical tests such as nitrogen utilisation, catalase, methyl red (M.R.), citrate utilisation, starch and gelatin hydrolysis were performed according to 'Bergey's Manual of Systematic Bacteriology' (Vos et al. 2009).

2.5 | Growth Curves

BSG and BSS were grown in 100 mL LB medium in a 250-mL Erlenmeyer flask and cultured at 37°C and 200 rpm on a rotary shaker. Growth curves were monitored by measuring the OD_{600} values.

2.6 | Biofilm Formation Assay

2.6.1 | Crystal Violet Stain

BSG and BSS were incubated in a 96-well cell culture plate at 37°C for 48 h. Each well was washed thrice with ultrapure water and stained with 0.1% crystal violet for 15 min. After the crystal violet staining, each well was washed thrice with methanol. Finally, the crystal violet bound to the biofilm was dissolved with 200 μL of methanol for 30 min, and absorbance at 590 nm was measured to determine the adhesion of formed biofilm using a microtiter plate reader.

2.6.2 | CLSM and COMSTAT Analysis

To observe the biofilm morphology, biofilm was grown in a sterile Confocal dish with 2 mL of sterile LB broth. After incubating at 37°C for 48 h, the used medium in the well of the plate was gently removed and washed three times with PBS (pH = 7.2) to eliminate free-floating bacteria. A viability staining kit was utilised to stain the live and dead cells in *B. subtilis* biofilms, containing a green fluorescent stain SYTO9, which penetrates both live and dead cells, and a red fluorescent stain propidium iodide, which has the capacity only to penetrate dead cells (Shailaja et al. 2022). A freshly prepared stain solution was pipetted to cover the entire biofilm. Confocal images were acquired by confocal laser scanning microscopy (CLSM). All single 2D sections of biofilms were obtained with a *z*-step of 1 μm between each *xy* image for *z*-stack under excitation wavelengths from 488 to 561 nm. Artificially coloured images of biofilm structure were then obtained using ImageJ software. CLSM images were analysed using the computer program COMSTAT 2.1 to quantify the morphological characteristics of biofilm structures (Heydorn et al. 2000).

2.7 | Secondary Metabolism Extraction and Analysis

2.7.1 | Fermentation Condition

BSG and BSS were cultivated in a fermentation medium containing (g/L): sucrose 20.00, KH_2PO_4 2.45, Na_2HPO_4 3.97, NH_4Cl 1.34, $NaNO_3$ 2.125, $MgSO_4$ 0.10, yeast extract 1.00, $CaCl_2$ 7.77×10^{-3} and $MnCl_2$ 12.58×10^{-3}. All fermentation experiments were performed at 37°C and 200 rpm for 72 h under aerobic conditions.

2.7.2 | Identification and Quantitative Analysis

After obtaining the cell-free broth, the supernatant was adjusted to a final pH of 2.0 by adding 6 mol/L HCl and then stored overnight at 4°C. The acid precipitate was obtained by centrifugation at 8000 rpm for 10 min and dried at 65°C to detect the yield of lipopeptide (Fei et al. 2020). After extracting the precipitate three times with diethyl ether, the organic phase was dried by air blowing to obtain the crude lipopeptide. Preliminary identification was performed by thin layer chromatography (TLC) and ESI-MS. The lipopeptide was dissolved in HPLC-grade acetonitrile, and then HPLC and LC–MS were used to quantitatively detect surfactins.

2.7.3 | Surface Activity Assays

The cell-free broth was obtained by centrifugation of the above culture at 8000 rpm for 20 min. The supernatant was adjusted to a final pH of 7.2 for the following experiments. The surface tension (SFT) was measured at 25°C ± 0.1°C with the plate method using a DCAT 21 tensiometer (DataPhysics, German). The pH was adjusted within the range of 4.0–12.0 with HCl and NaOH to evaluate the effect of pH on growth. The effect of salt concentrations was measured by adding NaCl until the final concentrations of 0%–20% (w/v). Also, to examine the effect of temperature, the cell-free broth was kept at different temperatures from 20°C to 120°C for 2 h and then cooled to room temperature. The surface tension versus concentration plot was used to determine critical micelle concentration (CMC) and minimum surface tension (γ_{CMC}). Equal volumes of cell-free broth and liquid paraffin were mixed by a vortex mixer for 1 min. The resulting mixture was incubated at 25°C for 24 h and then the emulsification index value (E_{24}) was calculated using the formula:

$$E_{24} = \frac{\text{Height of emulsion layer}}{\text{Height of the total mixture}} \times 100\,\%$$

2.8 | Genome Sequencing and Analysis

BSG and BSS were aerobically cultured in LB medium at 37°C for 20 h, then the cells were collected by centrifugation at 10000 rpm for 15 min. Then, the genomic DNA was extracted and purified using the PowerSoil DNA Isolation Kit (MO BIO, USA). The genome sequences were obtained with the second-generation platform Illumina sequencing according to standard protocols; the gene function annotation was achieved by homologous comparison with the reference sequence to the Clusters of Orthologous Group of proteins (COG, http://www.ncbi.nlm.nih.gov/COG/), Gene Ontology (GO, http://www.geneontology.org/) and Kyoto Encyclopedia of Genes and Genomes (KEGG, http://www.kegg.jp) Database (Chen et al. 2017; Galperin et al. 2019; Kanehisa et al. 2021). Annotated gene sequences were blasted using the Carbohydrate Active Enzyme Database (CAZy, http://bcb.unl.edu/dbCAN2/). Secondary metabolite biosynthesis gene clusters in BSG and BSS were detected using antiSMASH (http://antismash.secondarymetabolites.org) (Blin et al. 2023).

2.9 | Transcriptome Sequencing and Analysis

Total RNA was extracted from BSG and BSS using the Trizol RNA extraction method, and the ribosomal RNA was removed by the Epicentre Ribo-Zero rRNA Removal Kit; then, library construction was performed by the NEBNext Ultra II Directional RNA Library Prep Kit for Illumina. Finally, the Illumina-qualified libraries were sequenced on a high-throughput sequencing platform for PE150 sequencing and raw reads were generated. RSEM package was used to calculate FPKM (fragments per kilobase of transcript per million) values, and the differentially expressed genes (DEGs) were detected by edgeR among the compared groups, which were

significantly enriched with differential genes based on |log-2Fold Change| ≥ 1 and FDR ≤ 0.05. The biological functions and metabolic pathways of DEGs were determined based on the functional annotation data from GO and KEGG pathway analysis by clusterProfiler software, with the significance cut-off for FDR set at 0.05. The raw data of DNA-Seq and RNA-Seq were deposited in the National Center for Biotechnology Information (NCBI) database under accession numbers PRJNA1071808.

2.10 | Statistical Analysis

Quantification methods for the various parameters are described in the relevant Methods Section. Statistical analyses were performed using Microsoft Excel 2021. All experiments were repeated at least three times, and the results are presented as the mean ±standard error.

3 | Results

3.1 | The Physiological and Biochemical Characterisation

Growth curves of BSG and BSS strains based on the optical density at 600 nm (OD_{600}) exhibited similar growth properties during a 36-h incubation experiment (Figure 1A). However, the OD_{600} values demonstrated that the cell density and growth rate of BSS were relatively smaller compared with BSG within the first 24 h. Conversely, when entering the stationary growth phase, the cell concentration of BSS continued to be significantly

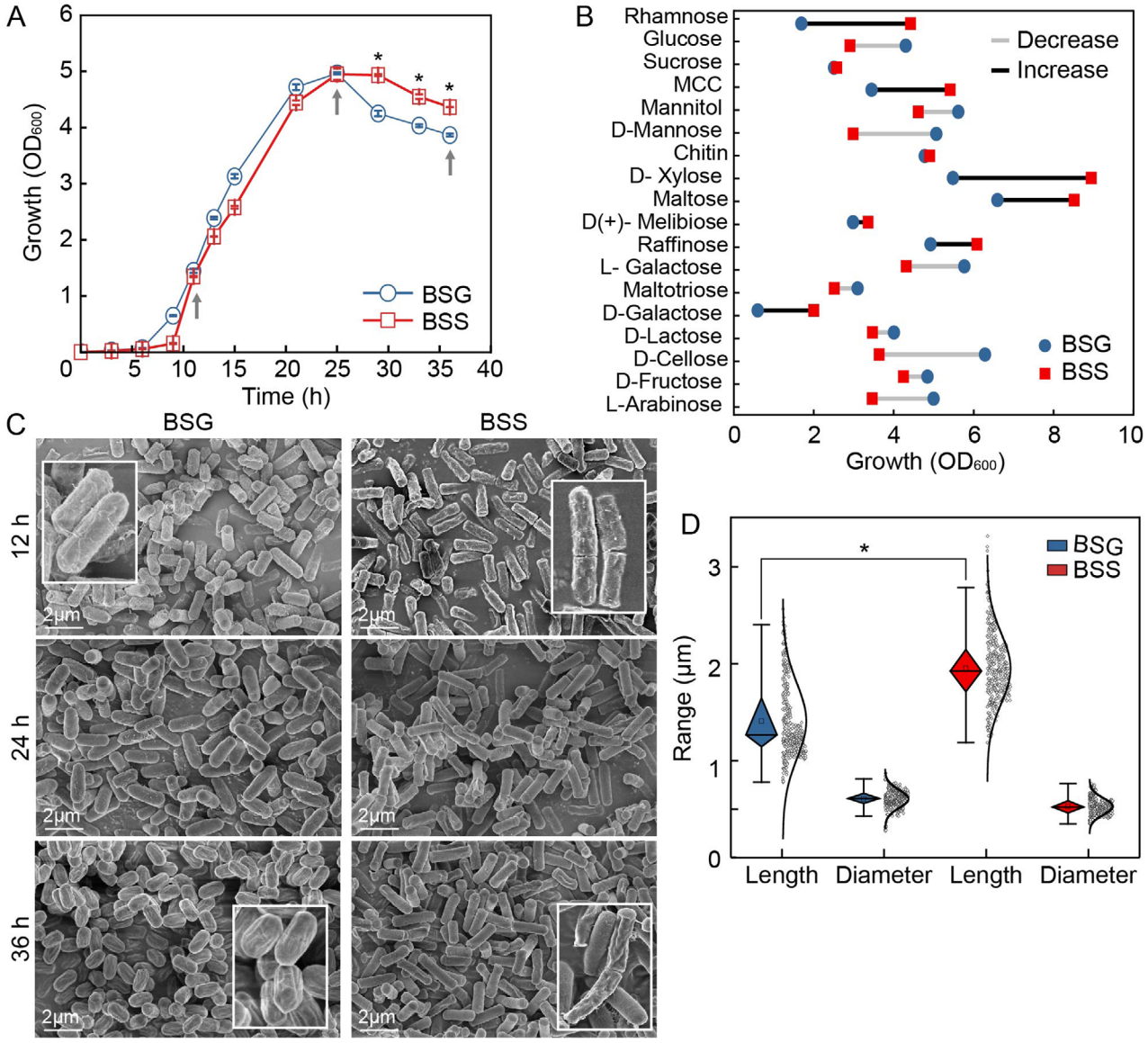

FIGURE 1 | Phenotypic characteristics of *B. subtilis*. (A) Growth curves of BSS and BSG cultured in LB medium at 37°C. The grey arrows (12, 24 and 36 h) on the growth curves indicated the sampling time points for observing morphology. (B) The sole-carbon-sources utilisation preference test with 18 carbon sources. (C) SEM images of morphology at three time points (12, 24 and 36 h) during the growth process. The scale bar is 2 μm. A white box in each picture means a partially enlarged view. The images are representative of three biological replicates. (D) Boxplot for average diameter and length based on SEM images. *Indicates a significant difference ($p < 0.01$).

higher, resulting in a 10% increase in the final cell concentration. Moreover, among 36 physiological and biochemical tests, significant differences in growth tolerance and motility tests were observed, in which BSS showed lower motility and stronger salinity tolerance up to 15% compared with the 10% of BSG (Table S1). In addition, the sole-carbon-source utilisation results revealed different carbon source preferences (Figure 1B). BSS exhibited significantly increased growth only in six carbon sources, including D-galactose, raffinose, maltose, D-xylose, MCC and rhamnose, while impaired growth in the remaining nine carbon sources.

Three time points at different growth stages were selected to investigate the changes in morphology: early logarithmic growth phase (12 h), plateau phase (24 h) and the end of the decline phase (36 h). Compared with the BSG cells, BSS cells showed an obvious difference in morphology at different stages, with a rougher surface at 12 h and 36 h and a smoother surface at 24 h (Figure 1C). In addition, the average cell size and size distribution were measured based on SEM images at the above three time points, indicating a significant increase in average length of BSS ($1.95 \pm 0.35\,\mu m$) compared with BSG cells ($1.41 \pm 0.38\,\mu m$) (Figure 1D).

3.2 | Biofilm Formation Assay

The ability to form biofilm is an important feature of *Bacillus sp.* associated with environmental adaptability and virulence. Therefore, we preliminarily evaluated the ability of BSG and BSS to form biofilm after 48 h of static cultivation. For the spaceflight-exposed strain BSS, the floating pellicle without wrinkling on the surface was observed, whereas BSG formed a robust biofilm with vigorous wrinkling (Figure 2A). CLSM analysis further confirmed the weaker biofilm formation ability after spaceflight. BSG biofilm structure was dense with obvious cell aggregations in the central and corner regions. In contrast, BSS showed a uniform biofilm distribution with many voids (Figure 2A). This result was consistent with the results of the crystal violet staining test. Further quantitative analysis revealed a significant decrease in the biomass, maximum thickness and average thickness of the entire area of BSS, which decreased 1.37-, 1.43- and 1.52-fold, respectively (Figure 2B). The above results demonstrated that the spaceflight inhibited biofilm formation by decreasing biofilm biomass and thickness.

3.3 | Secondary Metabolites Analysis

Lipopeptide is an important secondary metabolite of *B. subtilis* that exhibits great surface activity and biological activities (Chen et al. 2015). As previously reported, the crude extracts purified from cell-free broth were primarily characterised by TLC and ESI-MS (Figures S1 and S2), which were confirmed as a cyclic lipopeptide named surfactin (Figure 3A). The growth of two strains was regularly detected during 72-h fermentation cycle, with BSS showing a significantly lower cell concentration compared to BSG (Figure 3B**)**. Correspondingly, the surfactin production of BSS decreased, as evidenced by the HPLC yield of 0.145 g/L, which was 72.06% lower than that of BSG (Table 1). Nevertheless, the surface activity of surfactins produced by BSG and BSS, including surface tension, emulsification (E_{24}), CMC values and γ_{CMC}, was not significantly different (Figure 3C and Table 1). Additionally, the purified surfactins showed good stability when exposed to different temperatures (20°C–120°C), pH (4–12) and NaCl concentration (0%–20%). No significant difference was observed between BSG- and BSS-derived surfactin, with a stable ability to reduce the surface tension from 72 mN/m to around 28 mN/m (Figure 3D).

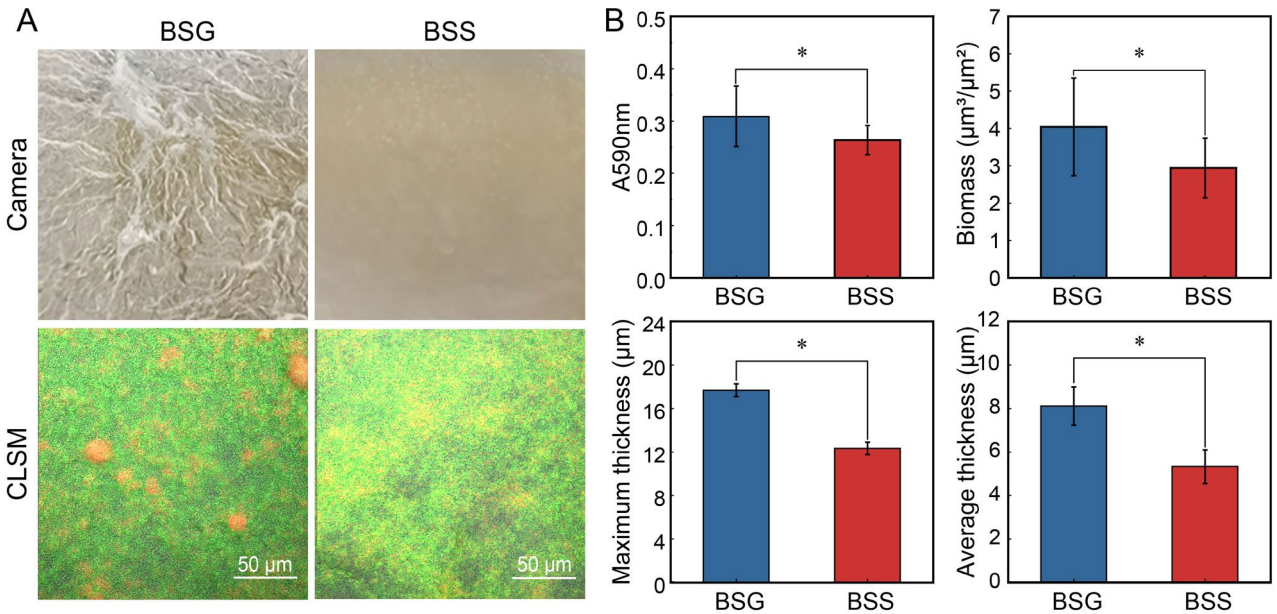

FIGURE 2 | The biofilm formation of *B. subtilis* after spaceflight. (A) The biofilm structure after static cultivation for 48 h was observed by a digital camera and CLSM. The scale bar is 50 μm. The image is representative of three biological replicates. (B) Quantitative analysis of biofilm formation assays and structural features. Quantitative calculation by crystal violet staining and COMSTAT analysis (biomass, maximum thickness and average thickness). Significant difference ($p < 0.01$) between BSG and BSS is denoted with*.

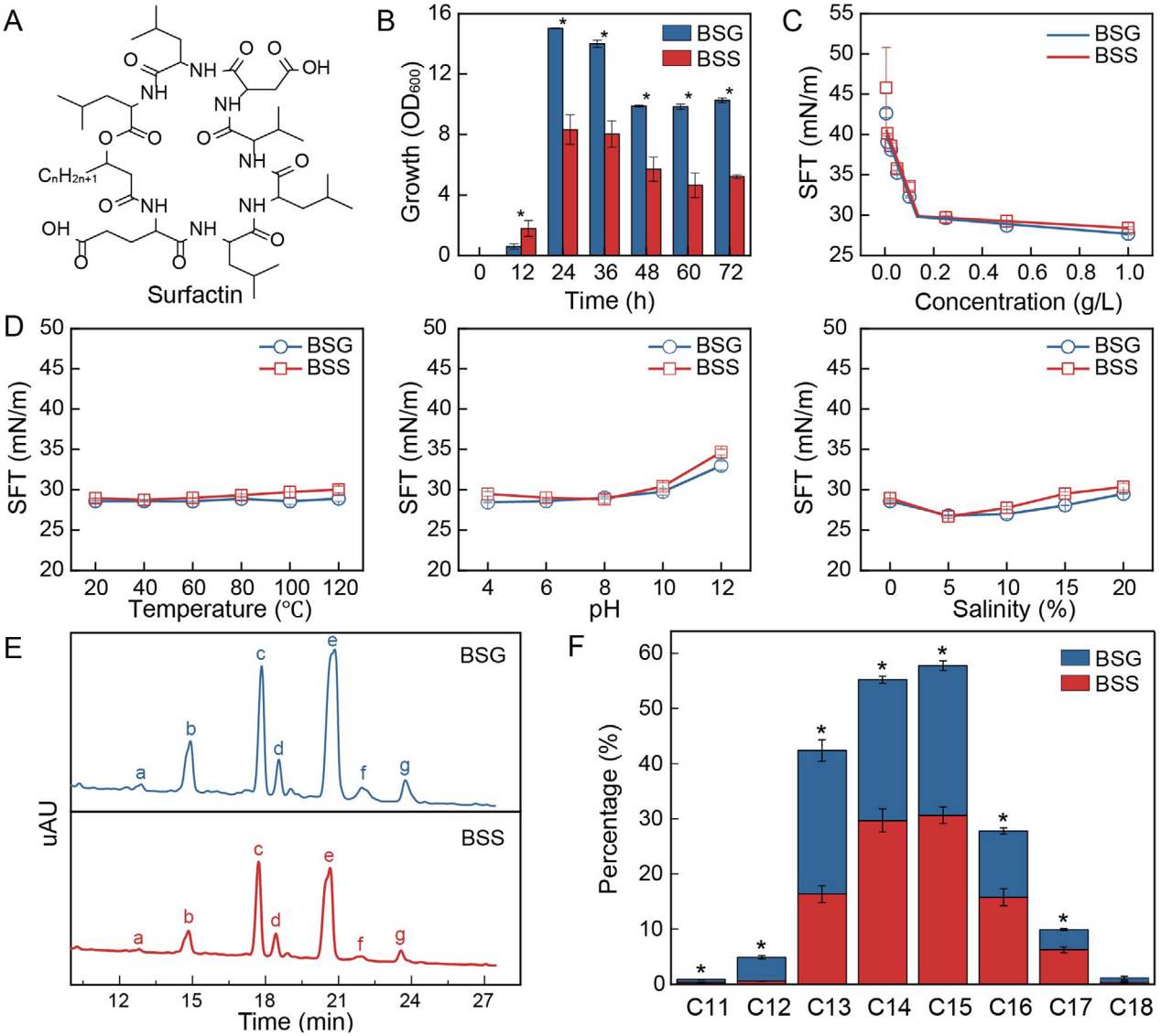

FIGURE 3 | Comparison of secondary metabolism between BSG and BSS. (A) Chemical structures of surfactin homologues. (B) The growth (OD_{600}) throughout the fermentation period. (C) Critical micelle concentration analysis of surfactins. (D Effect of environmental factors (temperature, pH and salinity) on the surface tension of fermentation broth. (E) HPLC chromatogram of surfactins extracted from the culture broth. Peaks a-g correspond to surfactin C12–surfactin C16. (F) Composition analysis of surfactin homologues with different fatty acid chains. Significant difference ($p < 0.01$) is denoted with*.

TABLE 1 | Yield and surface characteristics of crude lipopeptides produced by BSG and BSS.

Characteristics	BSG	BSS
Crude yield (g/L)	1.796 ± 0.265	1.696 ± 0.064
Yield in HPLC (g/L)	0.519 ± 0.154	0.145 ± 0.017
CMC (g/L)	0.1269	0.1349
γ_{CMC} (mN/m)	29.80	29.88
E24 (%)	56.3 ± 0.5	48.4 ± 1.3

Moreover, the surfactins obtained from microorganisms have been reported to be a mixture of surfactin homologues with different fatty acid chains (11–18 carbon atoms). Therefore, the composition of surfactin homologues produced by BSG and BSS was tentatively determined by HPLC. As shown in Figure 3E, Peaks a, b, c (d), e (f) and g corresponded to surfactin C12 ~ C16 (constitutional isomers), respectively. A significant decrease in the yield of all surfactin homologues was determined by calculating the peak area due to the reduced surfactin production. Since the amount of surfactin-C11, C17 and C18 was too small to be detected by HPLC, LC–MS was used for further analysis of the difference between the surfactin homologues. Molecular ion peaks at m/z $[M+H]^+ = 980$, 994, 1008, 1022, 1036, 1050, 1064 and 1078 were assigned to surfactin-C11 ~ C18, respectively, with hydrophobic chain lengths differing by 14 Da corresponding to a $-CH_2$ group (Figure S3). Normalised calculation of surfactin homologues revealed that there was a significant increase of surfactin homologues with longer hydrophobic chains (C14, C15, C16 and C17), which were increased from 25.8%, 28.1%, 12.6% and 3.4% to 29.8%, 31.3%, 15.2% and 6.3%, respectively (Figure 3F).

However, the number of surfactin homologues with shorter hydrophobic chains (C11, C12 and C13) significantly reduced to approximately 0%, 0.5% and 16.4%, respectively. Comparison results demonstrated that the surfactin homologues content of BSS was significantly different from that in BSG, further indicating that spaceflight has altered lipopeptide metabolism, both in the surfactin yield and composition.

3.4 | Genomic Analysis

Genomic analysis of the wild-type and spaceflight-exposed strains was performed to elucidate the influence of spaceflight on *B. subtilis*. Briefly, the complete genome sequence of BSG was composed of a circular chromosome of 4,070,924 bp, containing 4187 coding sequences (CDS) with an average G + C content of 43.81%, while the genome of BSS was 4,070,127 bp. The whole genome sequencing statistics were shown in Table S2, and the complete genomes were presented in the form of a circular graph, including genome sequences, protein CDS, RNA genes, GC content and GC skew (Figure 4). Further genomic analysis was performed by antiSMASH to screen for gene clusters involved in secondary metabolite biosynthesis. In total, 14 gene clusters for the biosynthesis of surfactin, fengycin and other bioactive compounds (Class II) were detected both in BSG and BSS (Table S3). The surfactin biosynthetic gene cluster (NRPS) was characterised in both BSG and BSS with 82% similarity of nucleotide sequence identity, which were presented from 349,747 to 413,186 and from 349,755 to 413,194, respectively. These clusters were comprised of core biosynthetic, additional biosynthetic, transport-related, regulatory and other genes, which further indicated the ability of BSG and BSS to produce surfactin and other bacteriostatic compounds. Interestingly, cluster 14 was identified in both strains and displayed only low similarity (10%) with the known gene cluster responsible for biosynthesis of thailanstatin A.

3.5 | Comparative Transcriptome Analysis

The comparative transcriptome analysis was carried out to investigate the influence of spaceflight on *B. subtilis* by analysing global changes in gene expression through four steps, including RNA sample extraction, detection, library construction and sequencing, with three biological replicates (Gong et al. 2021). The transcriptomic difference between the spaceflight-exposed group and the control group was represented visually by a volcano plot and unsupervised hierarchical clustering (Jakab et al. 2022). A total of 997 significant DEGs were detected, including 724 downregulated DEGs and 273 upregulated DEGs (Figure 5A,B). To gain better insight into which biological processes were significantly changed by spaceflight, GO and KEGG pathways were associated with the analysed DEGs. A total of 997 DEGs were associated with 26 GO entries, and most of the significantly upregulated genes that were influenced by spaceflight were enriched in the cellular anatomical entity, catalytic activity and metabolic process, while the significantly downregulated genes were mainly associated with a cellular anatomical entity, cellular process and catalytic activity (Figure 5C). We also performed pathway enrichment analysis by KEGG, and it turned out that spaceflight influenced 137 KEGG pathways in *B. subtilis* TD7 and two-component system, starch and sucrose metabolism, amino sugar and nucleotide sugar metabolism, butanoate metabolism and phosphotransferase system (PTS) had the top 5 number of genes with significant changes in the transcriptome (Figure 5D).

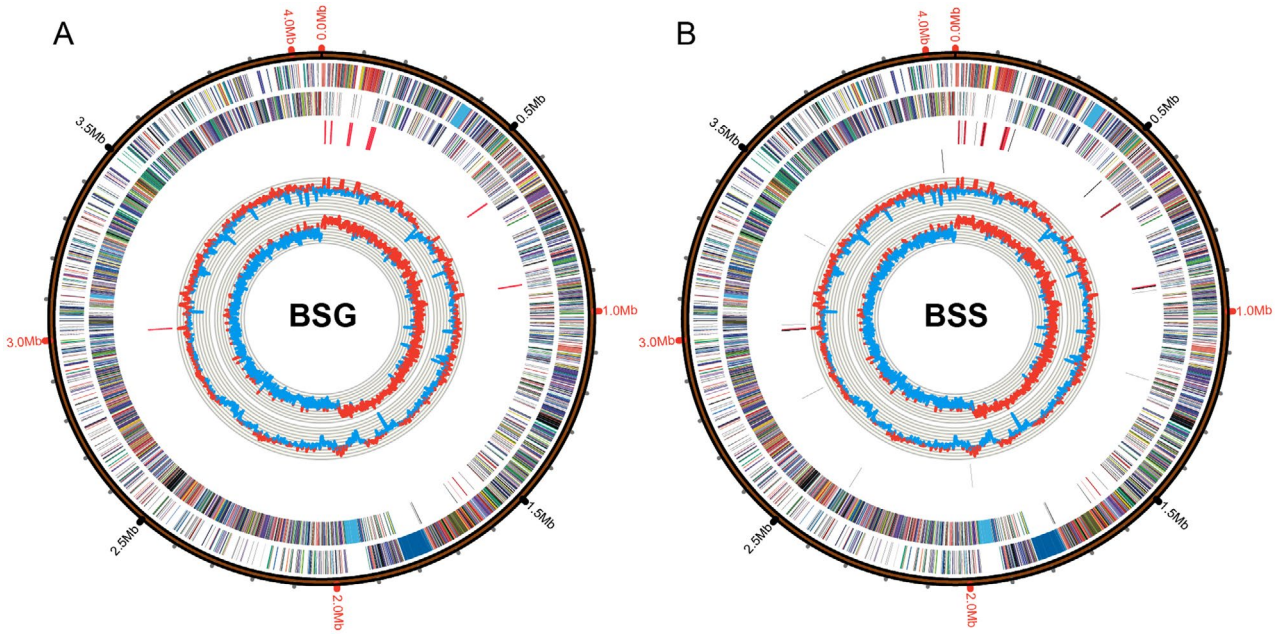

FIGURE 4 | Circular genome map of BSG (A) and BSS (B). From the outermost to the centre, Ring 1 for scale marks of the genome, Ring 2 for protein-coding genes on the forward strand, Ring 3 for protein-coding genes on the reverse strand, Ring 4 for tRNA (black) and rRNA (red) genes on the forward strand, Ring 5 for tRNA (black) and rRNA (red) genes on the reverse strand, Ring 6 for GC content and Ring 7 for GC skew. Protein-coding genes are colour-coded according to their COG categories.

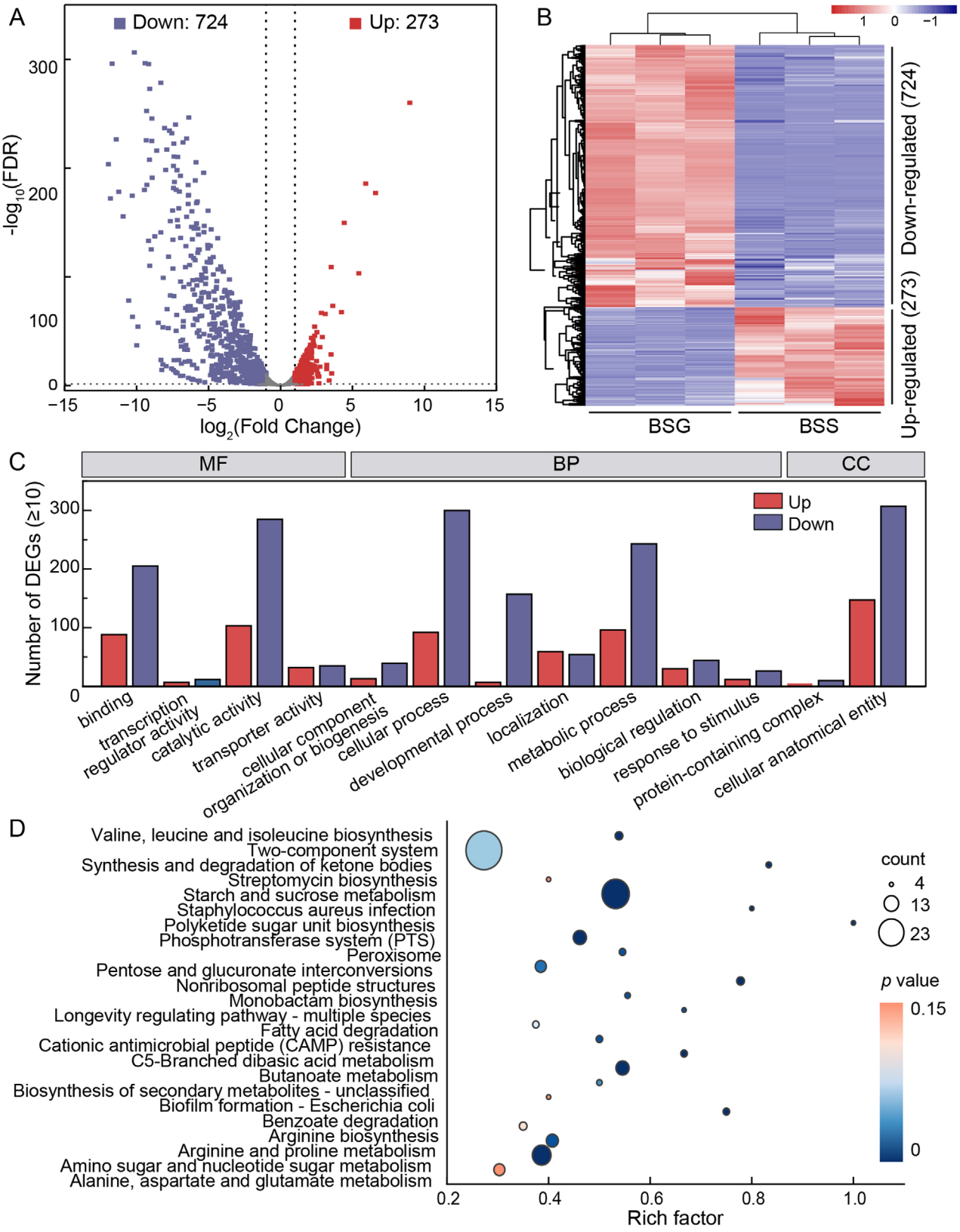

FIGURE 5 | Identification of differentially expressed genes (DEGs) induced by spaceflight. The cutoff values $|\log_2 \text{Fold change}| \geq 1$ and $\text{FDR} \leq 0.05$ were utilised to identify DEGs. (A) Volcano plot for the comparison of DEGs between BSG and BSS. Each dot represents a gene: Red, blue and grey colours are indicative of upregulated, downregulated and nonchanged genes, respectively. (B) Heat plot of DEGs generated from hierarchical cluster analysis of genes with each row representing a different gene. (C) Distribution of upregulated and downregulated DEGs of more than 10 based on GO functional annotation. MF for molecular function, BP for biological processes and CC for cellular components. (D) DEGs in the main KEGG pathways.

Spaceflight influenced multiple KEGG pathways associated with surfactin synthesis, including amino acid biosynthesis, nonribosomal peptide structures, TCA cycle, fatty acid degradation, starch and sucrose metabolism pathways, pyruvate metabolism and quorum sensing (Figure 6 and Table S4). There were six downregulated DEGs (*alsS, ilvC, leuA, leuB, leuC* and *leuD*) related to fatty acid biosynthesis and 16 downregulated DEGs related to amino acid biosynthesis, including valine, leucine and isoleucine biosynthesis (*leuA, leuB, leuC, leuD, alsS, ilvC* and *ilvH*), alanine, aspartate and glutamate

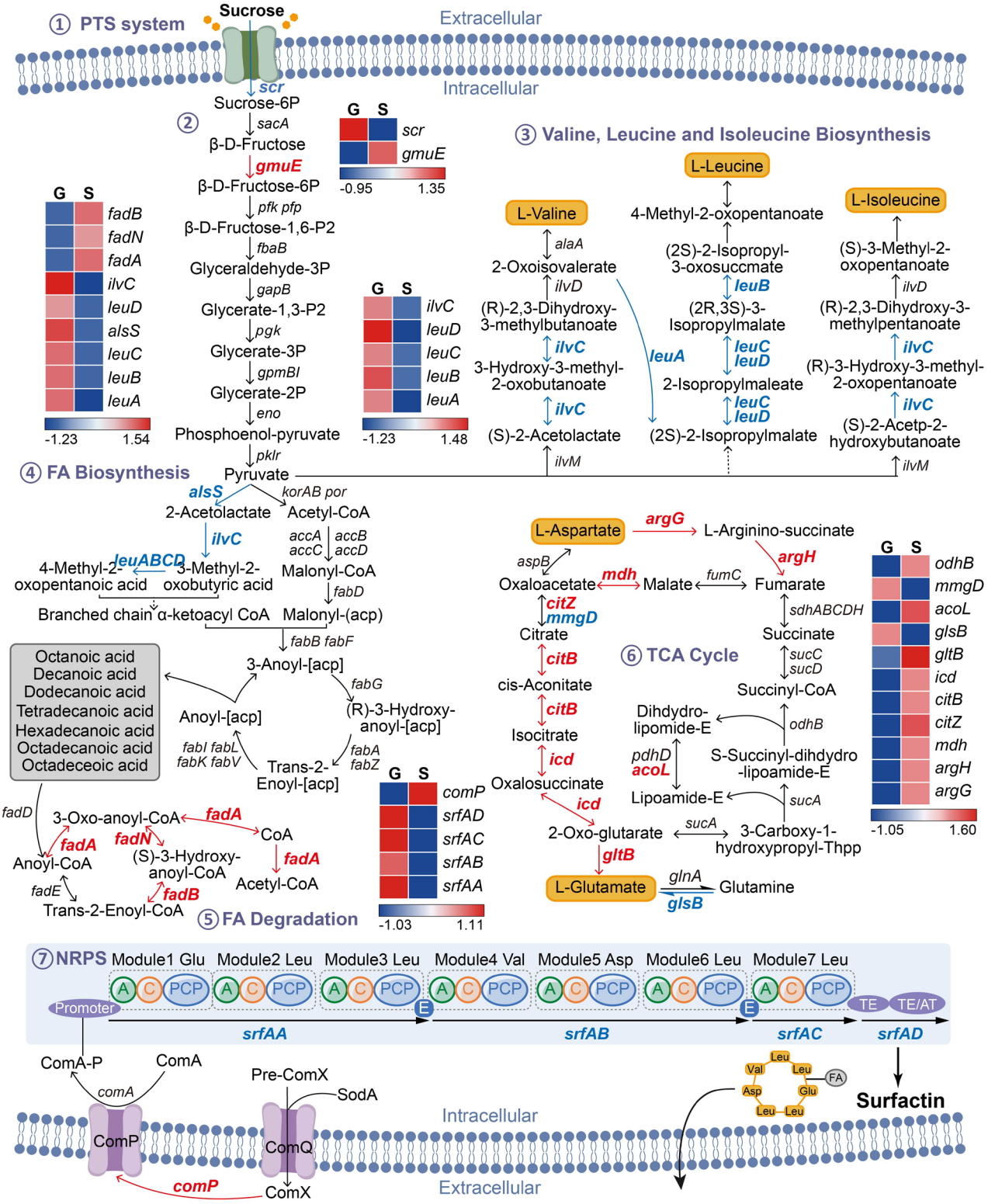

FIGURE 6 | The effect of spaceflight on surfactin biosynthesis pathways. Global comparison of KEGG pathways involved in surfactin synthesis. Upregulated and downregulated genes and nonchanged DEGs are written in red, blue and black, respectively. Orange represents amino acids associated with surfactin biosynthesis. The dashed line represents multiple-step reactions.

metabolism (*ansZ, glsB, nadB* and *asnO*) and glycine, serine and threonine metabolism (*dapG, gbsA, asd, gbsB* and *mccB*). However, we also detected one downregulated DEG (*mmgD*) and six upregulated (*icd, citZ, citB, acoC, acoL* and *mdh*) DEGs involved in the biosynthesis of glutamate and aspartate. Additionally, some key genes associated with surfactin synthesis were found to be significantly differentially expressed in BSS, including seven downregulated DEGs (*degU, degQ, comK, srfAA, srfAB, srfAC* and *srfAD*) and two upregulated DEGs (*sodA* and *comP*). Moreover, three DEGs involved in fatty acid degradation (*fadA, fadN* and *fadB*) were significantly upregulated, which has negative effects on accumulating lipid moieties for surfactin synthesis. Starch and sucrose metabolism pathways-related genes *gmuE* and *gapB* were significantly upregulated, and then the pyruvate metabolism process was activated. While pyruvate metabolism-related genes (*leuA, ldeHA, lgeHB* and *mmgA*) were significantly downregulated, leading to downregulation of fatty acid synthesis, and thus inhibiting surfactin synthesis. Also, DEGs (*aprE, comK, degU, nprB, pelA, srfAA, srfAB, srfAC, srfAD, vpr* and *yjbA*) related to quorum sensing were significantly downregulated.

4 | Discussion

4.1 | Phenotype Change Response for Spaceflight

Over the past few decades, many studies have reported that microorganisms exhibit a variety of phenotypic, resistance and virulence changes adapting to the extreme conditions of the space environment (Sheet et al. 2020; Su et al. 2021). In this work, we have comprehensively investigated the phenotypic changes in *B. subtilis* in response to spaceflight. In terms of microbial growth, there is still no definitive conclusion as to whether spaceflight has a positive or negative effect on growth. In this study, we found that BSS had a lower growth rate in the logarithmic phase and achieved a 10% higher cell density in the decline phase. Some previous studies have observed the increased growth of *Streptomyces coelicolor* after spaceflight (Huang et al. 2015), while others have shown no significant change between the space and control groups, such as *B. subtilis* (Fajardo-Cavazos et al. 2018), or even decreased cell density, such as *Deinococcus radiodurans* and *Mycobacterium marinum* (Abshire et al. 2016; Ott et al. 2020). The space environment has been known to have an impact on morphological transformations, including the extrusion and filamentation of colonies (Nielsen et al. 2021). In our study, there were significant changes in the morphological characteristics, which exhibited significantly longer cell lengths and stronger adherent abilities compared to BSG. This result may be explained by the fact that the expression of a gene, *dinK*, related to the cell division inhibitor, was significantly upregulated based on the transcriptomic analysis. There are two possible explanations for the increased cell density. First, the cell density data was obtained based on the optical density reading, meaning that both the number and size of cells can affect the results. Second, the significantly upregulated gene, *psdB*, may be responsible for the increase. Previous research has demonstrated that deletion of the *psdB* gene caused severe growth defects and that *psdB* played a critical role in hyphal growth (Takagi et al. 2021). Moreover, changes in growth are considered to be related to the culture medium, motility and bacterial species, which accords with previous observations that BSS exhibited decreased motility in biochemical tests. In addition, BSS exhibited preference differences for carbon source utilisation. Both strains could utilise 18 tested carbon sources, while BSS showed weaker growth except for D-galactose, raffinose, maltose, D-xylose, MCC and rhamnose. In general, it can be suggested that these phenotypic changes in morphology, motility and carbon source preference could be an adaptive response to some extreme stress, allowing *B. subtilis* to better adapt to environmental changes.

4.2 | Biofilm Formation Response for Spaceflight

B. subtilis is capable of forming robust and sophisticated biofilms, and this ability is closely related to adhesion, antibiotic resistance, pathogenicity and persistence in the face of environmental stress (Has et al. 2023; Lin et al. 2022). This is the first spaceflight study to evaluate the space-induced biofilm formation of *B. subtilis*, as previous aerobiological studies have primarily focused on pathogenic microorganisms. In this study, the space significantly impaired biofilm formation and adhesion ability in *B. subtilis*, showing a smoother surface and increasing voids. In contrast to the findings in the Biofilm Organisms Surfing Space experiment, where Frösler et al. (Frösler et al. 2017) suggested that *D. geothermalis* acquired biofilm formation ability after a 16-month low Earth orbit travel, and Billi et al. (Claudia et al. 2021) found that the overall resistance of biofilms formed by planktonic organisms to extreme conditions was higher, suggesting increased viability and lower amounts of DNA damage. Our COMSTAT analysis concluded that spaceflight affected the biofilm biomass and thickness, thus affecting the biofilm architecture. Consistent with our results, other studies also demonstrated that the alternation of strain motility contributed to biofilm development (Zhang et al. 2018). Furthermore, as in most previous experiments, there is a strong relationship between biofilm and surfactin production in many *Bacillus* species. As observed by Lopez et al. (López et al. 2009), surfactin was shown to trigger biofilm formation by causing intracellular potassium leakage sensed by KinC (sporulation sensor kinase C) to activate the biological synthesis pathways of biofilm formation (Xu et al. 2019). Taken together, the current results indicated that the difference in biofilm formation altered by spaceflight was likely due to the combination of the reduction in movement and surfactin production.

4.3 | Metabolic Pathways and Regulatory Mechanisms Response for Spaceflight

B. subtilis has the potential to produce a wide variety of natural products, and lipopeptides are well-known metabolites with excellent surface and biological properties. Among these, surfactin, a cyclic lipopeptide consisting of a hydrophobic chain and a lactone ring, is the most studied. According to our previous reports, lipopeptides derived from *B. subtilis* TD7 have been demonstrated to have great surface activity and are composed of many structural homologues (including surfactin C11 ~ C17) (Qin et al. 2023). BSS exhibited a slower growth with lower cell concentration in the culture process, which may result in inhibited secondary metabolism. HPLC analysis also revealed that the yield of surfactins decreased from 0.519 to 0.145 g/L. In addition, spaceflight affected

the relative amounts of homologues with different fatty acids in BSS, with an increase in homologues with longer fatty acids (14, 15, 16 and 17 carbon atoms) while a decrease in shorter fatty acids (11, 12 and 13 carbon atoms). Stability and performance under extreme conditions are essential factors of biosurfactant activities for industrial applications under complex environments, while no significant difference in the stability and surface activity of surfactins was observed. Due to the extremely low yield of surfactin in BSS, the difference in relative amounts of surfactin homologues with longer fatty acid chains did not significantly change the surface activity and stability of surfactins.

Whole genome sequencing of BSG and BSS was performed to further investigate the spaceflight effects. A total of 14 potential gene clusters encoding secondary metabolites were found in the genomes of BSG and BSS, indicating that both BSG and BSS have great potential for antimicrobial applications. Another interesting genomic feature is that a new gene cluster with low similarity to known clusters was detected, which is likely to yield novel natural products that may be undetected under standard fermentation conditions (Frikha-Dammak et al. 2021). Further work is required to investigate the effect of spaceflight on the identification and expression of other BGCs apart from NRPS via gene-editing methods. The availability of the genome sequences of the wild-type strain and spaceflight-exposed strain provides a framework for biotechnological analysis and characterisation of new natural products.

On the other hand, comparative transcriptomic analysis revealed that the global changes in gene expression of BSS were significantly different from the ground strain BSG. Genes with transcript levels 2-fold change (FC) >1 and FDR <0.05 were selected to identify DEGs in the spaceflight-exposed group. A total of 997 genes were differentially regulated in *B. subtilis* under spaceflight conditions, out of which 724 genes were significantly upregulated and 273 genes were significantly downregulated compared to the control group. Based on GO analysis, a large proportion of DEGs in BSS were involved in a variety of metabolic pathways, including cellular anatomical entity, catalytic activity and metabolic process. Furthermore, KEGG analysis showed that many genes that were differentially expressed in BSS included two-component system, PTS, starch and sucrose metabolism, butanoate metabolism and pentose and glucuronate interconversion. Thus, it can be suggested that spaceflight has exhibited great environmental adaptability in response to space stress through regulating membrane transport, carbohydrate metabolism and amino acid metabolism, especially the regulation of signal transduction.

Previous studies have revealed that *B. cereus* responded to the space environment through differential regulation of genes and proteins relevant to metabolism (Su et al. 2014). This study is the first to demonstrate that spaceflight has a pronounced impact on the secondary metabolism process of lipopeptide production and to elucidate the mechanism underlying the decrease in surfactin production based on comparative transcriptomic analysis. Surfactin synthesis was accomplished by NRPSs, which mainly involves three steps: the synthesis of fatty acid chain, the activation and loading of fatty acids and the extension of the peptide chain (Qi et al. 2023). Fatty acid synthesis plays a critical role in lipopeptide synthesis and gene expression levels are positively correlated with lipopeptide yield (Deng et al. 2022; Gao et al. 2022). Previous studies have proved that strengthening branched-chain fatty acid biosynthetic pathways was an efficient approach to enhancing lipopeptide yield (Qiao et al. 2024). In this study, no significant change in key genes was investigated in the fatty acid biosynthesis pathway involved in surfactin biosynthesis, while DEGs (*fadA, fadB* and *fadN*) related to fatty acid degradation were significantly upregulated, which was not conducive to the accumulation of fatty acid precursors leading to a decrease in surfactin production. To date, the effect of the regulation of amino acid metabolism on surfactin production has not yet been clear. In this study, spaceflight influenced multiple amino acid metabolic pathways in BSS, including alanine, aspartate, glutamate metabolism and valine, leucine and isoleucine biosynthesis. A decrease in genes (*leuA, leuB, leuC, leuD* and *ilvC*) involved in the metabolism of L-leucine and L-valine resulted in a decrease in amino acid precursors (Leu and Val) for surfactin biosynthesis. This is probably the reason why BSS synthesises low levels of surfactin. In addition, some DEGs (*argG* and *gltB*) associated with other amino acid precursors (Asp and Glu) for surfactin biosynthesis were significantly upregulated. This supports the findings of other studies, showing that the individual and combined inhibition of three genes (*yrpC*, *racE* and *murC*) related to L-glutamate metabolism improved surfactin production (Wang et al. 2019). As a result, we infer that the upregulated genes of *argG and gltB* might lead to decreased surfactin yield. Surfactin is biosynthesised by the NRPS system, and the *srfA* operon is specific to the synthesis of surfactin, which contains four open reading frames to code surfactin synthetase. *SrfAA* and *srfAB* are responsible for three amino acid assemblies (Leu, Glu, Val and Asp, Val and Leu), respectively; *srfAC* is responsible for the seventh amino acid assembly (Leu) and coding the first TE domain in order to terminate elongation of the peptide chain and peptide release; and *srfAD* encodes the second TE domain to activate peptide cyclisation (Sreedharan et al. 2023). ComA is also a key factor for regulating surfactin biosynthesis, which is regulated by ComQXP, RapC, SodA and DegQ (Théatre et al. 2021). Surfactin-producing genes, including *srfAA, srfAB, srfAC* and *srfAD*, were significantly downregulated in BSS, indicating that the key step of surfactin synthesis, the peptide chain extension, was significantly inhibited, thereby resulting in a drastically decreased surfactin yield. The inhibition effect was also observed in the pathway from pyruvate to 3-anoyl[acp]. The network and correlation analysis also provided valuable information about potential regulatory mechanisms of surfactin production in the space environment, which will be explored and verified in further studies. In addition, DEGs (*aprE, comK, degU, nprB, pelA, srfAA, srfAB, srfAC, srfAD, vpr* and *yjbA*) related to quorum sensing were significantly downregulated. Previous studies have demonstrated that quorum sensing can trigger the synthesis of surfactin (Oslizlo et al. 2014). The downregulated genes involved in quorum sensing inhibited the accumulation of surfactin. Also, surfactin can in turn function as a quorum-sensing molecule for biofilm formation in *B. subtilis*, thus decreased surfactin can result in a reduction of biofilm formation (Cui et al. 2012). Overall, this network included a downregulation of fatty acid biosynthesis, amino acid biosynthesis and NRPS process; upregulation of fatty acid degradation; and some amino acid biosynthesis inconducive to improving surfactin production, which works together to lead to a lower yield of surfactin.

5 | Conclusion

This study focused on investigating the effects of spaceflight on *B. subtilis* and the underlying metabolic mechanisms. Many phenotypic changes were observed in the spaceflight-exposed strain, including higher cell density, longer cell size, altered morphology, weaker biofilm-forming ability and secondary metabolism ability. Moreover, our results revealed the potential mechanisms underlying the altered lipopeptide metabolism after spaceflight, which were accomplished via increased fatty acid degradation, decreased amino acid biosynthesis, and NRPS process. These molecular strategies can inhibit not only the absorption and utilisation of the carbon source but also the biosynthesis of the precursor substrates for lipopeptide synthesis. Conclusively, this study on the influence of spaceflight on *B. subtilis* has enhanced our understanding of the biosynthetic and regulatory mechanisms of producing lipopeptides. These findings are expected to provide a new reference for future genetic engineering and synthetic biology to develop high-yield bacteria.

Author Contributions

Wan-Qi Qin: writing – original draft, writing – review and editing, formal analysis, methodology, data curation. **Yi-Fan Liu:** writing – review and editing, software. **Jin-Feng Liu:** resources, project administration. **Lei Zhou:** conceptualization. **Shi-Zhong Yang:** methodology, validation, supervision. **Ji-Dong Gu:** writing – review and editing. **Bo-Zhong Mu:** writing – review and editing, supervision, funding acquisition, conceptualization.

Acknowledgements

This work was supported by the National Key Research and Development Program of China (No. 2022YFC2105200), the Fundamental Research Funds for the Central Universities of China and the Research Program of the State Key Laboratory of Bioreactor Engineering. The authors thank the China Manned Space Program for carrying out our samples and the Research Centre of Analysis and Test of East China University of Science and Technology for the help on ESI-MS and CLSM analyses.

Conflicts of Interest

The authors declare no conflicts of interest.

Data Availability Statement

The data that support the findings of this study are available from the corresponding author upon reasonable request.

References

Abshire, C. F., K. Prasai, I. Soto, et al. 2016. "Exposure of *Mycobacterium Marinum* to Low-Shear Modeled Microgravity: Effect on Growth, the Transcriptome and Survival Under Stress." *npj Microgravity* 2: 16038.

Bijlani, S., E. Stephens, N. K. Singh, K. Venkateswaran, and C. C. C. Wang. 2021. "Advances in Space Microbiology." *iScience* 24: 102395.

Blin, K., S. Shaw, H. E. Augustijn, et al. 2023. "antiSMASH 7.0: New and Improved Predictions for Detection, Regulation, Chemical Structures and Visualisation." *Nucleic Acids Research* 51: W46–w50.

Chen, L., Y. H. Zhang, S. Wang, Y. Zhang, T. Huang, and Y. D. Cai. 2017. "Prediction and Analysis of Essential Genes Using the Enrichments of Gene Ontology and KEGG Pathways." *PLoS One* 12: e0184129.

Chen, W.-C., R.-S. Juang, and Y.-H. Wei. 2015. "Applications of a Lipopeptide Biosurfactant, Surfactin, Produced by Microorganisms." *Biochemical Engineering Journal* 103: 158–169.

Claudia, M., F. Claudia, N. Alessandro, R. Elke, R. Petra, and B. Daniela. 2021. "Revival of Anhydrobiotic Cyanobacterium Biofilms Exposed to Space Vacuum and Prolonged Dryness: Implications for Future Missions Beyond Low Earth Orbit." *Astrobiology* 21: 541–550.

Cockell, C. S., P. Rettberg, E. Rabbow, and K. Olsson-Francis. 2011. "Exposure of Phototrophs to 548 Days in Low Earth Orbit: Microbial Selection Pressures in Outer Space and on Early Earth." *ISME Journal* 5: 1671–1682.

Coil, D. A., R. Y. Neches, J. M. Lang, et al. 2016. "Growth of 48 Built Environment Bacterial Isolates on Board the International Space Station (ISS)." *PeerJ* 4: e1842.

Cui, Y., Y. Zhao, Y. Tian, W. Zhang, X. Lü, and X. Jiang. 2012. "The Molecular Mechanism of Action of Bactericidal Gold Nanoparticles on *Escherichia Coli*." *Biomaterials* 33: 2327–2333.

Daniela, B., S. Clelia, V. Cyprien, et al. 2019. "Dried Biofilms of Desert Strains of Chroococcidiopsis Survived Prolonged Exposure to Space and Mars-Like Conditions in Low Earth Orbit." *Astrobiology* 19: 1008–1017.

Deng, Q., H. Lin, M. Hua, et al. 2022. "LC-MS and Transcriptome Analysis of Lipopeptide Biosynthesis by *Bacillus Velezensis* CMT-6 Responding to Dissolved Oxygen." *Molecules* 27: 6822–6833.

Dergham, Y., D. Le Coq, P. Nicolas, et al. 2023. "Direct Comparison of Spatial Transcriptional Heterogeneity Across Diverse *Bacillus subtilis* Biofilm Communities." *Nature Communications* 14: 7546.

Fajardo-Cavazos, P., J. D. Leehan, and W. L. Nicholson. 2018. "Alterations in the Spectrum of Spontaneous Rifampicin-Resistance Mutations in the *Bacillus Subtilis* rpoB Gene After Cultivation in the Human Spaceflight Environment." *Frontiers in Microbiology* 9: 192.

Fei, D., F. F. Liu, H. Z. Gang, et al. 2020. "A New Member of the Surfactin Family Produced by *Bacillus subtilis* With Low Toxicity on Erythrocyte." *Process Biochemistry* 94: 164–171.

Frikha-Dammak, D., H. Ayadi, I. Hakim-Rekik, L. Belbahri, and S. Maalej. 2021. "Genome Analysis of the Salt-Resistant Paludifilum Halophilum DSM 102817T Reveals Genes Involved in Flux-Tuning of Ectoines and Unexplored Bioactive Secondary Metabolites." *World Journal of Microbiology and Biotechnology* 37: 178.

Frösler, J., C. Panitz, J. Wingender, H. C. Flemming, and P. Rettberg. 2017. "Survival of *Deinococcus Geothermalis* in Biofilms Under Desiccation and Simulated Space and Martian Conditions." *Astrobiology* 17: 431–447.

Galperin, M. Y., D. M. Kristensen, K. S. Makarova, Y. I. Wolf, and E. V. Koonin. 2019. "Microbial Genome Analysis: The COG Approach." *Briefings in Bioinformatics* 20: 1063–1070.

Gao, L., M. She, J. Shi, et al. 2022. "Enhanced Production of Iturin A by Strengthening Fatty Acid Synthesis Modules in *Bacillus amyloliquefaciens*." *Frontiers in Bioengineering and Biotechnology* 10: 974460.

Gong, M., H. Zhang, D. Wu, et al. 2021. "Key Metabolism Pathways and Regulatory Mechanisms of High Polysaccharide Yielding in Hericium Erinaceus." *BMC Genomics* 22: 160.

Has, E. G., N. Akçelik, and M. Akçelik. 2023. "Comparative Global Gene Expression Analysis of Biofilm Forms of *Salmonella Typhimurium* ATCC 14028 and Its seqA Mutant." *Gene* 853: 147094.

Heydorn, A., A. T. Nielsen, M. Hentzer, et al. 2000. "Quantification of Biofilm Structures by the Novel Computer Program Comstat." *Microbiology* 146: 2395–2407.

Huang, B., D. G. Li, Y. Huang, and C. T. Liu. 2018. "Effects of Spaceflight and Simulated Microgravity on Microbial Growth and Secondary Metabolism." *Military Medical Research* 5: 18–32.

Huang, B., N. Liu, X. Rong, J. Ruan, and Y. Huang. 2015. "Effects of Simulated Microgravity and Spaceflight on Morphological

Differentiation and Secondary Metabolism of *Streptomyces Coelicolor* A3(2)." *Applied Microbiology and Biotechnology* 99: 4409–4422.

Jakab, Á., F. Kovács, N. Balla, et al. 2022. "Physiological and Transcriptional Profiling of Surfactin Exerted Antifungal Effect Against *Candida albicans*." *Biomedicine & Pharmacotherapy* 152: 113220.

Juhas, M., and J. W. Ajioka. 2017. "T7 RNA Polymerase-Driven Inducible Cell Lysis for DNA Transfer From *Escherichia Coli* to *Bacillus Subtilis*." *Microbial Biotechnology* 10: 1797–1808.

Kanehisa, M., M. Furumichi, Y. Sato, M. Ishiguro-Watanabe, and M. Tanabe. 2021. "KEGG: Integrating Viruses and Cellular Organisms." *Nucleic Acids Research* 49: D545–D551.

Krüger, A., N. Welsch, A. Dürwald, et al. 2022. "A Host-Vector Toolbox for Improved Secretory Protein Overproduction in *Bacillus subtilis*." *Applied Microbiology and Biotechnology* 106: 5137–5151.

Lam, K. S., S. W. Mamber, E. J. Pack, S. Forenza, P. B. Fernandes, and D. M. Klaus. 1998. "The Effects of Space Flight on the Production of Monorden by *Humicola Fuscoatra* WC5157 in Solid-State Fermentation." *Applied Microbiology and Biotechnology* 49: 579–583.

Lin, Y., R. Briandet, and Á.,. T. Kovács. 2022. "*Bacillus Cereus* Sensu Lato Biofilm Formation and Its Ecological Importance." *Biofilms* 4: 100070.

López, D., M. A. Fischbach, F. Chu, R. Losick, and R. Kolter. 2009. "Structurally Diverse Natural Products That Cause Potassium Leakage Trigger Multicellularity in *Bacillus Subtilis*." *PNAS* 106: 280–285.

Lu, J. Y., K. X. Zhou, W. T. Huang, et al. 2019. "A Comprehensive Genomic and Growth Proteomic Analysis of Antitumor Lipopeptide Bacillomycin Lb Biosynthesis in *Bacillus Amyloliquefaciens* X030." *Applied Microbiology and Biotechnology* 103: 7647–7662.

Mora, M., L. Wink, I. Kögler, et al. 2019. "Space Station Conditions Are Selective but Do Not Alter Microbial Characteristics Relevant to Human Health." *Nature Communications* 10: 3990.

Mu, B.-Z., F.-F. Liu, Y.-F. Liu, et al. 2021. "Improvement Surfactin Production by Substitution of Promoters in *Bacillus Subtilis* TD7." *Applied Environmental Biotechnology* 6: 11.

Nielsen, S., K. White, K. Preiss, et al. 2021. "Growth and Antifungal Resistance of the Pathogenic Yeast, *Candida Albicans*, in the Microgravity Environment of the International Space Station: An Aggregate of Multiple Flight Experiences." *Life (Basel)* 11: 283.

Oikawa, H., Y. Mizunoue, T. Nakamura, et al. 2022. "Structure and Biosynthesis of the Ribosomal Lipopeptide Antibiotic Albopeptins." *Bioscience Biotechnology and Biochemistry* 86: 717–723.

Oslizlo, A., P. Stefanic, I. Dogsa, and I. Mandic-Mulec. 2014. "Private Link Between Signal and Response in *Bacillus Subtilis* Quorum Sensing." *PNAS* 111: 1586–1591.

Ott, E., Y. Kawaguchi, D. Kölbl, et al. 2020. "Molecular Repertoire of *Deinococcus radiodurans* After 1 Year of Exposure Outside the International Space Station Within the Tanpopo Mission." *Microbiome* 8: 150.

Qi, X., W. Liu, X. He, and C. Du. 2023. "A Review on Surfactin: Molecular Regulation of Biosynthesis." *Archives of Microbiology* 205: 313.

Qiao, J., R. Borriss, K. Sun, et al. 2024. "Research Advances in the Identification of Regulatory Mechanisms of Surfactin Production by Bacillus: A Review." *Microbial Cell Factories* 23: 100.

Qin, W. Q., D. Fei, L. Zhou, et al. 2023. "A New Surfactin-C17 Produced by *Bacillus Subtilis* TD7 With a Low Critical Micelle Concentration and High Biological Activity." *New Journal of Chemistry* 47: 7604–7612.

Sani, A., W.-Q. Qin, J.-Y. Li, et al. 2024. "Structural Diversity and Applications of Lipopeptide Biosurfactants as Biocontrol Agents Against Phytopathogens: A Review." *Microbiological Research* 278: 127518.

Shailaja, A., T. F. Bruce, P. Gerard, R. R. Powell, C. A. Pettigrew, and J. L. Kerrigan. 2022. "Comparison of Cell Viability Assessment and Visualization of *Aspergillus Niger* Biofilm With Two Fluorescent Probe Staining Methods." *Biofilms* 4: 100090.

Sheet, S., S. Yesupatham, K. Ghosh, M. S. Choi, K. S. Shim, and Y. S. Lee. 2020. "Modulatory Effect of Low-Shear Modeled Microgravity on Stress Resistance, Membrane Lipid Composition, Virulence, and Relevant Gene Expression in the Food-Borne Pathogen *Listeria Monocytogenes*." *Enzyme and Microbial Technology* 133: 109440.

Sreedharan, S. M., N. Rishi, and R. Singh. 2023. "Microbial Lipopeptides: Properties, Mechanics and Engineering for Novel Lipopeptides." *Microbiological Research* 271: 127363.

Su, L. X., L. S. Zhou, J. W. Liu, et al. 2014. "Phenotypic, Genomic, Transcriptomic and Proteomic Changes in *Bacillus Cereus* After a Short-Term Space Flight." *Advances in Space Research* 53: 18–29.

Su, X., Y. Guo, T. Fang, et al. 2021. "Effects of Simulated Microgravity on the Physiology of *Stenotrophomonas Maltophilia* and Multiomic Analysis." *Frontiers in Microbiology* 12: 701265.

Takagi, K., A. Kikkawa, R. Iwama, R. Fukuda, and H. Horiuchi. 2021. "Type II Phosphatidylserine Decarboxylase Is Crucial for the Growth and Morphogenesis of the Filamentous Fungus *Aspergillus Nidulans*." *Journal of Bioscience and Bioengineering* 131: 139–146.

Théatre, A., C. Cano-Prieto, M. Bartolini, et al. 2021. "The Surfactin-Like Lipopeptides From Bacillus Spp.: Natural Biodiversity and Synthetic Biology for a Broader Application Range." *Frontiers in Bioengineering and Biotechnology* 9: 623701.

Vos, P. D., G. M. Garrity, D. Jones, et al. 2009. *Bergey's Manual of Systematic Bacteriology*. Springer.

Wang, C., Y. Cao, Y. Wang, L. Sun, and H. Song. 2019. "Enhancing Surfactin Production by Using Systematic CRISPRi Repression to Screen Amino Acid Biosynthesis Genes in *Bacillus Subtilis*." *Microbial Cell Factories* 18: 90.

Wu, Q., Y. Zhi, and Y. Xu. 2019. "Systematically Engineering the Biosynthesis of a Green Biosurfactant Surfactin by *Bacillus Subtilis* 168." *Metabolic Engineering* 52: 87–97.

Xu, Z., I. Mandic-Mulec, H. Zhang, et al. 2019. "Antibiotic Bacillomycin D Affects Iron Acquisition and Biofilm Formation in *Bacillus Velezensis* Through a Btr-Mediated FeuABC-Dependent Pathway." *Cell Reports* 29: 1192–1202.

Yang, R., S. Lei, X. Xu, et al. 2020. "Key Elements and Regulation Strategies of NRPSs for Biosynthesis of Lipopeptides by *Bacillus*." *Applied Microbiology and Biotechnology* 104: 8077–8087.

Zhang, J., J. He, C. Zhai, Z. Ma Luyan, L. Gu, and K. Zhao. 2018. "Effects of PslG on the Surface Movement of *Pseudomonas Aeruginosa*." *Applied and Environmental Microbiology* 84: e00219-00218.

Supporting Information

Additional supporting information can be found online in the Supporting Information section.